Chapter 5

Lift and drag in ideal fluids

We take up now the study of the effects of vorticity on ideal fluid flow. One of the most interesting and subtle properties of ideal fluid flow theory is its relation to the physical properties of real, viscous fluids as the viscosity tends to zero. We will consider viscous fluids in chapters 6-8. In the present chapter we shall need to comment on some aspects of the role of viscous stresses in determining the relevance of the ideal fluid and the applicability of Euler's equations when vorticity and circulation do not vanish.

Our main point is to draw a distinction between the *limit process flow* obtained from a real fluid flow in the limit of vanishing viscosity, and the *ideal fluid flow* theory which results from setting viscosity formally equal to zero. Because of the nature of the mathematical form of viscous stresses, involving the *spatial rate of change of the velocity*, viscous stresses can be non-negligible at arbitrarily small viscosity when the velocity changes sufficiently rapidly. In ideal fluid theory the fluid velocity is assumed to be tangent to any fixed solid boundary abutting the flow. If this surface undergoes rapid changes in slope, as at a corner, large viscous stresses can develop. To relieve these stresses the flow can change, and we shall give examples of this below. The effect can persist even as viscosity vanishes. In fact surfaces need not be present. The persistent effect of viscosity also occurs in fluid away from boundaries, when the fluid is in turbulent motion. In that case the small spatial scales come from the stretching of vortex tubes by the flow. When a rigid body moves rapidly through a fluid it will often create vorticity, which is then embedded in the otherwise irrotational flow, and we shall explore examples of this. These considerations lead to ideal flow models which incorporate the effects of the viscosity of the real fluid, despite the fact that viscosity has been expelled from the equations of motion. Since the theoretical basis for dealing precisely with limit process flows is not well developed, the models we will study are fairly crude approximations. Nevertheless they adequately capture the essential physics and have important applications.

The title of this chapter emphasizes the most important applications of these ideas, to the concepts of lift and drag in aerodynamics. A closely related problem

is the generation of thrust in flapping flight and by swimming fish. We begin with the calculation of lift of two-dimensional airfoils, then consider a model of a lifting three-dimensional wing. We also show in that case that drag is realized in an ideal (but not irrotational) fluid. Both lift and drag will be associated with vorticity. This vorticity may occur within a body, in which case it is called *bound vorticity*, or it may be in the flow exterior to the body, where it behaves as a material vector field. It is then called *free vorticity*. For a body moving with constant velocity through a quiescent ideal fluid can create a *vortical wake* stretching out behind it, a familiar example being the trailing vortices behind a high-flying jet. Vortical wakes are also creating by birds in forward flight, and by swimming fish.

It is easy to see how drag might be associated with a vortical wake. First we need to clarify these terms. *Drag* is conventionally equal to the component of force experienced by a body, parallel to the direction of motion. *Lift* is the component normal to the direction of motion, positive if opposite to gravity. If a body is pulled through the fluid with speed U and creates vorticity at a steady rate, this vorticity is carried off to infinity, and in the absence of viscosity there will be no decay. Consequently the associated flux of energy F_E is a loss to the system, which must be replenished by the work done against drag D, $UD = F_E$. A weightless self-propelled body in motion with constant average velocity is, according to Newton, not exerting any average force on the fluid. So in steady flight the drag must be balanced by thrust developed by a propeller, a jet engine, or a flapping fin. If the weight of a body minus the buoyancy (Archimedean) force is nonzero, then an unaccelerated body will exert a net force downward (against gravity) to compensate this net weight. The equilibrium can thus be expressed as thrust= drag and lift= weight in steady translation. In this case the energy in the vortical wake must equal to the work being done on the fluid by the body as it moves, to enable the flying or swimming, whether this is by a propeller, flapping wings, or a tail fin.

5.1 Lift in two dimensions and the Kutta-Joukowsky condition

In an ideal fluid any force on a two-dimensional body must be a result of the pressure exerted on the body. Accoring to the Bernoulli theorem for steady flow, the distribution of the pressure force over the surface of the body is directly related to the distribution of velocity there. This viewpoint can then lead to an attempt to understand the creation of lift as being a result of higher velocity over the top of the airfoil than over the bottom. Such an explanation, although mathematically correct, offers no hint of *why* the observed velocity distribution occurs.

To understand the basis of lift in two dimensions it is helpful to consider the simplest of "airfoils", namely a simple flat plate. Of course this choice is special since each end point of the plate is an extreme corner where the tangent

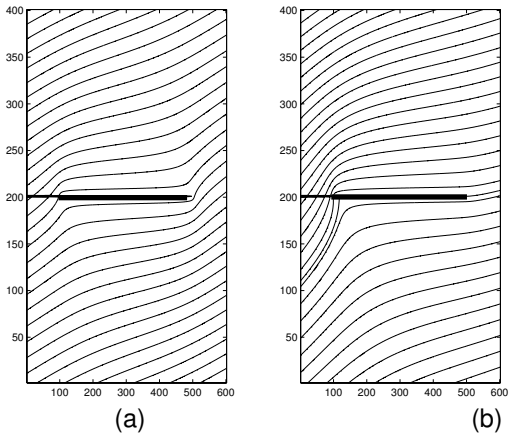

Figure 5.1: Streamlines for uniform flow past a flat plat, $\alpha = .2$. (a) Zero circulation. (b) Circulation determined by the Kutta-Joukowsky condition.

to the surface changes in direction by 180^o. We will later consider more realistic airfoils.

Now the circle of radius a into the Z-plane is mapped into the doubly-covered segment $|x| \leq 2a$ in the z-plane by $z = Z + a^2/Z$. We know also that uniform potential flow with velocity $(U, V) = Q(\cos\alpha, \sin\alpha)$ past the circular cylinder is not unique; the general solution is

$$W(Z) = Q[e^{-i\alpha}Z + a^2 e^{i\alpha}Z^{-1}] - \frac{i\Gamma}{2\pi}\ln Z, \tag{5.1}$$

where Γ is the circulation about the cylinder. With $w(z) = W(Z(z))$ we can then consider the streamline pattern about the plate for various Γ. The angle α, in the language of aeronautics, is called the *angle of attack* of the airfoil, here a flat plate.

We show in figure 5.1(a) the case of zero circulation $\Gamma = 0$. There are points of zero velocity, or *stagnation points* on the surface of the plate. The flow is forced around the endpoints so as to maintain the tangency of velocity at the body, and it is easy to see that there are singularities of velocity and pressure at $z = (\pm 2a, 0)$. In figure 5.1(b) we show the same flow with a negative Γ, chosen to move the stagnation point on the upper surface to the point $(2a, 0)$ and to eliminate the singularity there. The singularity at the point $(-2a, 0)$ remains.

We must now ask, what does one observe in a wind tunnel? Under conditions where ideal flow theory should prevail, except very close to the body surface, it is observed that the flow does come away smoothly from the downstream or "trailing" edge of the plate, as in figure 5.1(b). Experiments also show that the flow art the upstream or "leading" edge of the plate is actually as shown in figure 5.2, with *separation* of the boundary streamline at the leading edge, and reattachment further back, a small circulating eddy being enclosed by the separating streamline.

Figure 5.2: Leading-edge separation from a flat plate.

What we thus see is a definite upstream-downstream asymmetry of the flow in its response to the singular points of the boundary. [1] The flow seeks to make a smooth flow off the trailing edge, but accommodates itself on the leading edge by forming a separation bubble which effectively gives a smooth shape to the upstream end of the surface.

It can be assumed that this observed flow actually persists in the limit of arbitrarily small viscosity. In fact, hydrodynamic instabilities will generally prevent one from every observing the limit process as a steady flow, but the assumed limit would presumably apply to the unstable steady branch of solutions of the equations of the real fluid.

The condition which selects, among all possible values of Γ, the unique value which eliminates the singularity at the trailing edge of the plate, is called the *Kutta-Joukowsky condition*. To apply it in the present case, we note that

$$\frac{dw}{dz} = \Big[Q[e^{-i\alpha} - a^2 e^{i\alpha} Z^{-2}] - \frac{i\Gamma}{2\pi} Z^{-1}\Big] \frac{dZ}{dz}$$

$$= \Big[Q[e^{-i\alpha} - a^2 e^{i\alpha} Z^{-2}] - \frac{i\Gamma}{2\pi} Z^{-1}\Big] \Big[\frac{\sqrt{z^2 - 4a^2} + z}{2\sqrt{z^2 - 4a^2}}\Big]. \tag{5.2}$$

The terms within the first set of large brackets must sum to zero at $Z = a$ if the singularity at $z = 2a$ is to be removed. Thus we find

$$\Gamma = -4\pi Q a \sin\alpha \tag{5.3}$$

from the Kutta-Joukowsky condition. Once this condition is applied, the ideal flow theory matches the observations at the trailing edge, but fails to account for the separation bubble at the leading edge. This turns out not to be a serious discrepancy since the bubble acts to smooth the pressure distribution and mimic the smoothing of the airfoil leading edge.

To see that the resulting flow gives rise to a lift force, we compute the force on the body from Blasius' formula (4.14). From the residue of $(dw/dz)^2(z)$ we find (see problem 5.1(a))

$$X - iY = \rho\Gamma Q(\sin\alpha + i\cos\alpha). \tag{5.4}$$

This is a force of magnitude $L = 4\pi\rho a Q^2 \sin\alpha$, which is orthogonal to the free stream velocity for the geometry of figure 5.1(b), and is upward for positive α by (5.3) ($\Gamma < 0$) , so it is indeed a lift. It is *not* orthogonal to the plate itself,

[1] We shall see in chapter 8 that this asymmetry can be traced to the parabolic nature of the partial-differential equation for the viscous boundary layer on the surface of the body.

which raises the paradoxical situation where a pressure force, presumably always orthogonal to the surface, seems to be in violation of that fact. The resolution of this paradox involves a careful analysis of the singularity near the leading edge. The airfoils considered in the next section have a smooth leading edge, and the flate plate may be regarded as the limit of a family of such smoothed foils. Now for each member of the family, it is found that the pressure distribution around the smooth nose in fact produces a component of force parallel to the plate, which is precisely the magnitude needed to make the lift vector orthogonal to the free stream velocity. This "leading edge suction force" is preserved in the limit, even though the "edge" the disappears, and gives the result (5.4) for the flat plate.

Although the K-J condition gives a unique circulation and lift for an airfoil, it remains an approximation to reality. Rapid movements of an airfoil can produce momentary flows which differ from that obtained under the K-J condition, and may be close to the flow with zero circulation in figure 5.1(a). In fact the "true" K-J theory, which would allow the "correct" ideal flow representing the slightly viscous flow under arbitrary movements of a body, remains an important, outstanding unsolved problem of fluid dynamics, and lies at the heart of a rigorous theory of vortex shedding from surfaces.

5.2 Smoothing the leading edge: Joukowski airfoils

We have noted that the leading edge of a flat plate is not well suited to the smooth flow that we wanted to establish around an airfoil by the application of the Kutta-Joukowsky condition. Airfoil designers therefore prefer a shape which maintains the sharp trailing edge, so as to "force" the Kutta-Joukowsky condition there, but which also provides a smooth leading edge around which the flow may pass without detachment.

Remarkably, such foils can be obtained by a simple modification of the conformal map associated with the flat plate flow. Instead of considering flow around the circular cylinder of radius a and center at the origin, we consider the flow past a circular cylinder with center at $Z_0 = \epsilon + i\delta$ and radius $c = \sqrt{(a-\epsilon)^2 + \delta^2}$, with $\epsilon < 0, \delta > 0$. We show in figure 5.3 the foil shapes that result from various choices of ϵ, δ. Note that ϵ determines the foil thickness, and δ its *camber*, or the arc the foil makes relative to the x-axis. The geometry of the Z-plane is shown in figure 5.4. The trailing edge is a cusp.

It is not difficult to modify the force calculation to accommodate the Joukowsky family of profiles, and there results a lift force orthogonal to the free stream velocity, but with magnitude (see problem 5.1(b))

$$= 4\pi\rho c Q^2 \sin(\alpha+\beta), \tan\beta = \frac{\delta}{a-\epsilon}. \tag{5.5}$$

Note that the effect of camber is to change the angle of attack at which the lift vanishes.

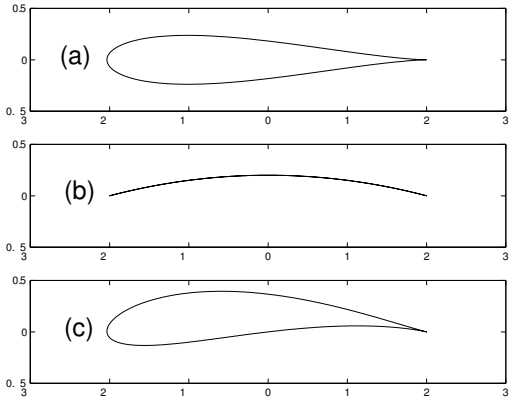

Figure 5.3: Joukowsky airfoils, a=1. (a) $\epsilon = -.1, \nabla = 0$ (b) $\epsilon = 0, \nabla = .1$ (c) $\epsilon = -.1, \nabla = .1$.

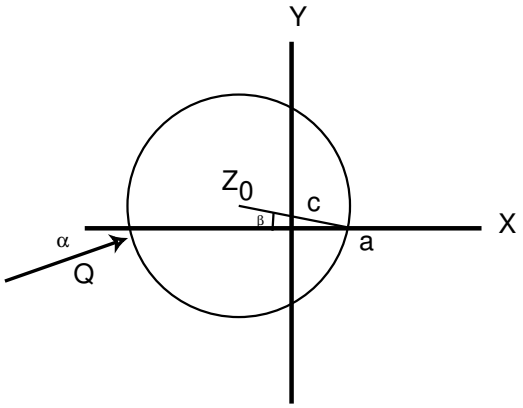

Figure 5.4: Geometry of the Z-plane for the Joukowsky airfoils. $Z_0 = \epsilon + i\delta$.

The moment on a Joukowsky airfoil can be computed by residue theory using the formula given in problem 4.3. To work this out we have

$$\Big(\frac{dw}{dz}\Big)^2 = \Big[Qe^{-i\alpha} - \frac{c^2}{z^2}Qe^{i\alpha} - \frac{i\Gamma}{2\pi z} - \frac{i\Gamma Z_0}{2\pi z^2}\Big]^2\Big[1 - \frac{a^2}{z^2}\Big]^2 +)(z^{-3}), \qquad (5.6)$$

and so the residue at infinity of $z(dw/dz)^2$ is $-2Q^2a^2e^{-21\alpha} - 2Q^2c^2 - \frac{i}{\pi}Q\Gamma Z_0 e^{-i\alpha} - \frac{1}{4\pi^2}\Gamma^2$. Thus

$$M = -\frac{1}{2}\rho\Re\Big[(2\pi i)\big[-2Q^2a^2e^{-2i\alpha} - 2Q^2c^2 - \frac{i}{\pi}Q\Gamma Z_0 e^{-i\alpha} - \frac{1}{4\pi^2}\Gamma^2\big]. \qquad (5.7)$$

After substituing $Z_0 = Z_0 - a + a = -ce^{-i\beta} + a$ we obtain

$$M = -2\pi\rho Q^2\big[a^2\sin 2\alpha + c^2\sin 2(\alpha+\beta) - 2ac\cos\alpha\sin(\alpha+\beta)\big]. \qquad (5.8)$$

Recall moment is positive in the counter-clockwise direction and (5.8) refers to a Joukowski airfoil with the trailing edge to the right. If $\beta = 0$ and α, δ are small, then $a \approx C$ and $M \approx -4\pi\rho Q^2a^2\alpha \approx -aL$. This places center of lift at approximately $z = -a$. The length of the foil, known as the *chord*, $\approx 4a$, so the center of lift is approximately at the quarter-chord point. For many aircraft the position of the center of gravity is is located near this point to provide stability to forward flight.

If one looks at wind tunnel data for Joukowsky airfoils, or for the many other foil designs of a similar kind, it is found that the predictions for lift at small angles of attack is reasonably good, especially in slope. Usually one plots a *lift coefficient* $C_L = \frac{L}{\frac{1}{2}\rho Q^2 4a}$ versus α. For the Joukowsky foils $C_L = 2\pi\frac{\sin(\alpha+\beta)}{\cos\beta}$. Realized lift is usually somewhat smaller than predicted. More dramatic is the failure of the theory to account for *airfoil stall*, a fall-off lift with increasing α, which usually begins for α in the range $10 - 15^o$. Stall is a result of separation of the flow from the foil, again a manifestation of the effects of viscosity. Usually the flow becomes unsteady as well, so an aircraft experiences buffeting and an abrupt loss of lift. Aircraft designers introduce modifications of three-dimensional wings, such as twist, reducing the angle of attack of outboard wing sections relative to inboard, to minimize the control problems and make the stall a more gradual phenomenon as angle of attack increases.

5.3 Unsteady and quasi-steady motion of an airfoil

Unsteady motion of an airfoil occurs during th take-off and maneuvering of an airplane, and in the flapping of the wings of birds and insects. A interesting thought experiment is to imagine an airfoil at positive angle of attack and leading edge to the left, to be suddenly accelerated from rest to the velocity $(-Q, 0)$. After the flow has settled down, and observer moving with the foil would see

a steady flow $(Q, 0)$ past the foil and would measure a lift, hence a circulation $\Gamma > 0$. Now repeat the experiment with a large material contour initially encircling the foil, see figure 5.5. The initial circulation on this contour is is zero since the fluid is at rest. After the acceleration to a fixed velocity, there exists a negative circulation about the foil. However, according to Kelvin's theorem, the circulation about the image of the large initial contour, now distorted by the motion of the foil, must remain zero. (The contour is a material curve.) Since we know the foil has negative circulation, there must be other vorticity within the contour contributing positive circulation. Observation of the acceleration of foils shows that this missing vorticity occurs at the initial acceleration of the foil. Positive vorticity is rapidly shed at the trailing edge, to form a coherent *starting vortex* whose circulation exactly cancels the circulation bound to the foil in steady flight, as we show in figure 5.5. This is an example of the *unsteady aerodynamics* of an airfoil. Such unsteady motions will generally involve shedding of vorticity from the trailing edge, and the shed vorticity will then influence the flow external to the foil. The shed vorticity moves with the fluid, and must be accounted for in calculating the forces on the foil.

A measure of unsteadiness is a parameter of the form $\frac{L}{TU}$ where L is some typical length, T a time over which a cycle of motion is performed, and U a speed of flight. If this dimensionless number is of order unity or larger, the the resulting flow is sqid to be fully unsteady. If the number is small, the flow is said to be *quasi steady*. A dragonfly may beat its wings once in $T = 1/40$ second and have a wing chord L=1 cm. If it moves at U=40 cm/sec then $\frac{L}{TU} = 1$ and the flow is unsteady. A pigeon with a wingbeat each 1/5 sec, a wing chord of 10 cm, flying at 3 m/sec has $\frac{L}{TU} = 1/6$, so its flight might be considered quasi-steady.

Let us devise a quasi-steady theory of forward fight of a flapping wing. While it is true that birds are flapping their wings to fly, the fact is that the main reason for flapping is to produce *thrust*, so as to overcome drag. A flapping Joukowsky airfoil at angle of attack $\alpha = -\beta$ produces only thrust. To acquire lift it is only necessary to increase the angle of attack while maintaining the flapping at that angle of attack. But of course to develop lift the wing must be moving! So the initiation of flappong flight is a kind of "bootstrap" operation where special wing movements may be needed.

To understand thrust production without any net lift consider a simple flat plate in uniform flow, which maintains itself horizontal while moving up and down in a periodic motion, see figure 5.6. Remember that as the plate moves we sshall assume quasi-steady aerodynamics, meaning that the *instantaneous* flow about the plate will be the steady flow corresponding to the instantaneous velocity the wing sees approaching it, and we assume the Kutta-Joukowsky condition applies. Thus in figure 5.6(a) the wing is moving down with speed V, and so sees an effective angle of attack $\alpha, \tan\alpha = V/U$. The "lift" vector $\mathbf{L}$ is orthogonal to this the instantaneous approach velocity vector (U, V), which produces a thrust component $T = L\sin\alpha = 4\pi a Q^2 \sin^2\alpha$. In fig 5.6(b) the wind moves up, but the same expression for thrust results. Thus the average in time of the thrust is positive, $\overline{T} = 4\pi a Q^2 \overline{\sin^2\alpha}$.

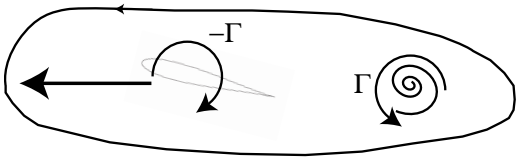

Figure 5.5: The starting vortex shed by a lifting foil abruptly accelerated to a constant velocity.

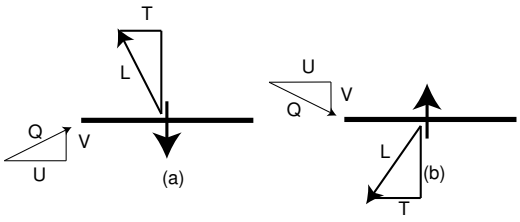

Figure 5.6: Thrust production by quasi-steady flapping of a flat plate.

We remark that in quasi-steady flapping flight there is a steady stream of vorticity shed from the the trailing edge of the foil, but it is swept downstream so fast that its effect on the flow is small.

5.4 Drag in two-dimensional ideal flow

In the present section we give two examples of the modeling of drag in an ideal fluid. Recall that for irrotational flow the drag force will vanish in two or three dimensions. In fact, a body in a real fluid will experience drag. We will see how drag in two-dimensional flow can result from vorticity in the fluid.

5.4.1 The Von Kármán vortex street

Experiments with flow past a circular cylinder in a wind tunnel, and numerical calculation in two dimensions, show that as the velocity of the stream increases, a point is reached where the flow becomes unsteady and vortices are shed into the flow, alternating between the top and bottom of the cylinder, see figure 5.7(a). These vortices (really patches of vorticity) are the carried by the flow downstream, forming a vortical wake. This wake carries energy downstream, and cylinder experiences a drag. The time dependence can give rise to an oscillating lateral force, and one manifestation is the "singing" of wires in a wind.

Von Kármán developed a simple model for such a wake, called now the *Kármán vortex street*. It consists of a periodic array of point vortices of strengths $\pm\gamma$, extending from the cylinder to downstream infinity. It can be most conveniently analyzed by extending the street to upstream infinity as well. So the

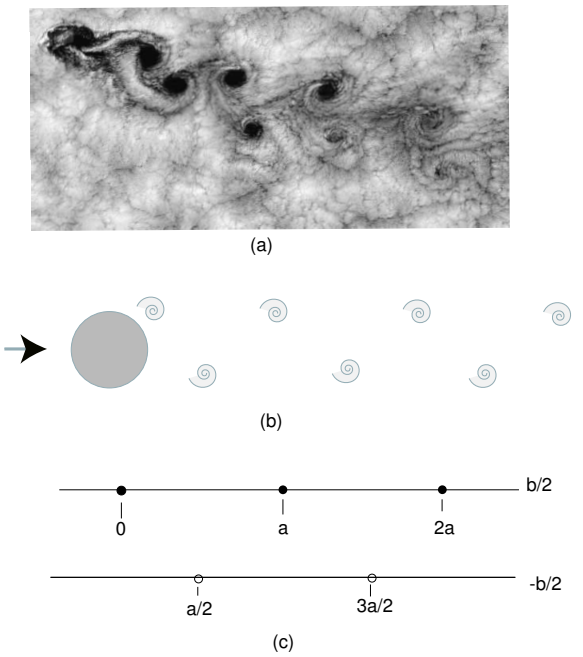

Figure 5.7: (a) Kármán vortex street in the atmosphere due to motion past an island off the Chilean coast. These atmospheric motions are very nearly two-dimensional. (b) Schematic of vortex shedding from a circular cylinder. (c) The doubly infinite street. The upper vortices carry circulation $-\gamma$. The lower vortices carry circulation $\gamma > 0$.

model is of the wake well downstream of the cylinder, see figure 5.7(b). The We show in figure 5.7(c) Von Kármán's doubly infinite vortex street. To study this flow, consider first a single finite line of vortices of circulation γ, spaced a distance a apart on the x-axis. The velocity potential is

$$w_N = -\frac{i\gamma}{2\pi}\sum_{n=-N}^{+N}\log(z-na) = -\frac{i\gamma}{2\pi}\log\Big[\frac{\pi z}{a}\Pi_{n=1}^{N}\big(1-\frac{z^2}{n^2a^2}\big)+\text{ constant}. \quad (5.9)$$

Using the identity

$$\sin z = z\big(1-\frac{z^2}{\pi^2}\big)\big(1-\frac{z^2}{2^2\pi^2}\big)\big(1-\frac{z^2}{3^2\pi^2}\big)\cdots, \quad (5.10)$$

we get, in the limit $N\to\infty$ for a suitable additive constant,

$$w_n \to w_\infty = -\frac{i\gamma}{2\pi}\log\sin\frac{\pi z}{a}. \quad (5.11)$$

For the vortex street shown in figure 5.7(c), we thus have

$$w_\infty = \frac{i\gamma}{2\pi}\log\Big(\frac{\sin\frac{\pi}{a}(z-ib/2)}{\sin\frac{\pi}{a}(z-a/2+ib/2)}\Big). \quad (5.12)$$

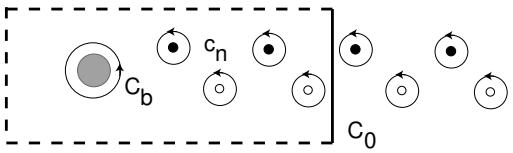

Figure 5.8: Contours for calculating drag for the vortex street.

Since the vortices are being shed by a body in a flow $(U, 0)$, relative to the body the complete velocity potential is

$$w = Uz + w_\infty. \tag{5.13}$$

Two see how the vortices are moving relative to an observer fixed with the body, we can, by symmetry, consider the velocity at $(0, b/2)$ for the system minus the votex at that point. Thus the vorticies move with velocity

$$\lim_{z \to ib/2} \left[\frac{dw}{dz} - \frac{i\gamma}{2\pi} \frac{1}{z - ib/2} \right] = U - V. \tag{5.14}$$

Evaluating this limit, we find

$$V = \frac{\gamma}{2a} \tanh \frac{\pi b}{a}. \tag{5.15}$$

In experiments V is considerably less than U, so the vortices move downstream with a speed slightly less than the free stream speed. For a circular cylinder of diameter D the vortices of like sign are shed with a frequency f where $fd/U \approx .2$. Thus $(U - V)/f = a \approx 5d$.

The drag force can be computed using the Blasius formula for force, but with an added effect due to the fact that vortices are being steadily added as they are shed from the body. We describe the ideas involved with this calculation without all the details. Relative to an observer *fixed with the vortex street* the velocity at infinity is V, the body is moving to the left with speed $U - V$. Imagine a rectangular boundary $C_0 = ABCD$ surrounding the the entire region, as shown in figure 5.8. The dotted sides will eventually move off move off to infinity and the solid line will be placed at a position far downstream where the street will be effectively doubly infinite. The small positively oriented contours c_n surround the vortices, and the contour C_b is the body contour. The side AB does not intersect any vortex. At a particular time the the Blasius theorem may be applied to yield

$$X - iY = -\oint_{\sum c_n} \left(\frac{dw}{dz} \right)^2 dz + \oint_{C_0} \left(\frac{dw}{dz} \right)^2 dz, \tag{5.16}$$

where the sum is over the c_n within C_0. In this frame the potential seen on AB,

$$w_V = Vz + w_\infty, \tag{5.17}$$

will be essentially independent of time of the street is taken as doubly infinite. The contributions from the first integral in (5.16) are seen to contribute only to Y, since the residues are just $2V\frac{\pm i\gamma}{2\pi}\gamma$. (These contributions would allow us to deduce an oscillating vertical force on the body.) The second term in (5.16) gets contribution in the limit only from AB and we obtain the following contribution to the drag from (5.16):

$$D_1 = \Re\frac{i\rho}{2}\int_{-i\infty}^{+i\infty}\Big(\frac{dw_V}{dz}\Big)^2 dz = \frac{\gamma^2\rho}{2\pi a}\Big(1 - \frac{\pi b}{a}\tanh\frac{\pi b}{a}\Big). \tag{5.18}$$

However there is also momentum being created as a function of time by the shedding of vortices within C_0. At this point we must do an approximate calculation, for the shed vortices break the symmetry of a doubly infinite street. We can approximate the calculation by determining the $x-$momentum per unit length of the street from w_∞, m say, then determining the momentum shed be cycle period T as ma/T. Since $(U-V)T = a$, the contribution will be $D_2 = -m(U-V)$ since positive drag contributes negative x-momentum.

To compute ma, we need only consider two adjacent vortices of opposite sign. Thus

$$ma = \rho\int\frac{dw_\infty}{dz}dS$$

$$= \rho\int_{-\infty}^{+\infty}dy\int_{-\infty}^{+\infty}\Big(\frac{i\gamma}{2\pi(x+iy-ib)} - \frac{i\gamma}{2\pi(x+iy-a/2+ib)}\Big)dx.$$

$$= \frac{i\rho\gamma}{2\pi}\int_{-\infty}^{+\infty}\big[\log(x+iy-ib) - \log(x+iy-a/2+ib)\big]_{x=-\infty}^{x=+\infty}dy. \tag{5.19}$$

Now the integrand in (5.19) gets contributions from the change of the argument of the log terms as x goes from $-\infty$ to $+\infty$. This is seen to give $+2\pi i$ when $|y| < b$ and zero when $|y| > b$. Thus we have

$$ma = -\rho\gamma b, \tag{5.20}$$

and

$$D_2 = \rho b\gamma(U-V)/a. \tag{5.21}$$

Thus the drag of the body is

$$D = D_1 + D_2 = \frac{\gamma^2\rho}{2\pi a}\Big(1 - \frac{\pi b}{a}\tanh\frac{\pi b}{a}\Big) + \rho b\gamma(U-V)/a$$

$$= \frac{\rho\gamma b}{a}(U-2V) + \frac{\rho\gamma^2}{2\pi a}. \tag{5.22}$$

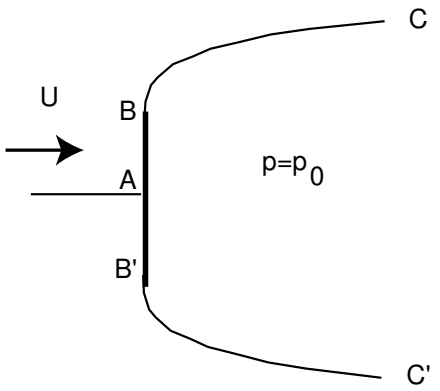

Figure 5.9: Free streamline flow onto a flat plate, a=1.

5.4.2 Free streamline theory of flow normal to a flat plate

There is another body of theory in two-dimensional ideal fluid flow involving streamlines on which velocity is discontinuous, and where these lines of discontinuity are embedded in the flow exterior to any boundaries. These *free streamline* theories effectively embed free vorticity in an otherwise irrotational flow field. Suppose that one one side of a streamline, as the streamline is approached, the velocity is non-zero, but on the other side the velocity is identically zero and pressure is constant. If the flow is steady and and Bernoulli's theorem applies then on the flow side $p + \frac{\rho}{2}|\mathbf{u}|^2$ is constant on the streamline. We now assert that at such a streamline pressure must be continuous. Otherwise a difference of pressure would act across a sheet, with no inertia to support such a force by a finite acceleration. Thus it must be that $|\mathbf{u}| = q$ is constant on the free streamline.

We will now examine a model, due to Kirchoff, which seeks to represent the detached flow that is observed behind bluff bodies in a uniform stream. The theory will deal with a steady flow, even though the observed flows are always time-dependent. The structure is shown in figure 5.9 in the case of flow broadside onto a finite flat plate. Two free separation streamlines leave the tips of the plate and extend to infinity aft of the body. The region behind the plate, between the free streamlines, is a cavity or "dead water" region, where velocity is zero and pressure a constant p_0. Well upstream the velocity is $(U, 0)$ and the pressure is p_0. Thus $p + \frac{\rho}{2}q^2 = p_0 + \frac{\rho}{2}U^2$ and in particular $q = U$ on the free streamlines.

Ths solution to this flow problem involves a interesting technique in conformal mapping, which exploit a correspondence between identical maps in distinct variables, allowing a direct connection between these variables and an equation determining the complex potential. The procedure is sometimes referred to as a *hodograph method* because the velocity components appear in the definition of an intermediate complex variable. We now describe the series of maps involved and the connections between them.

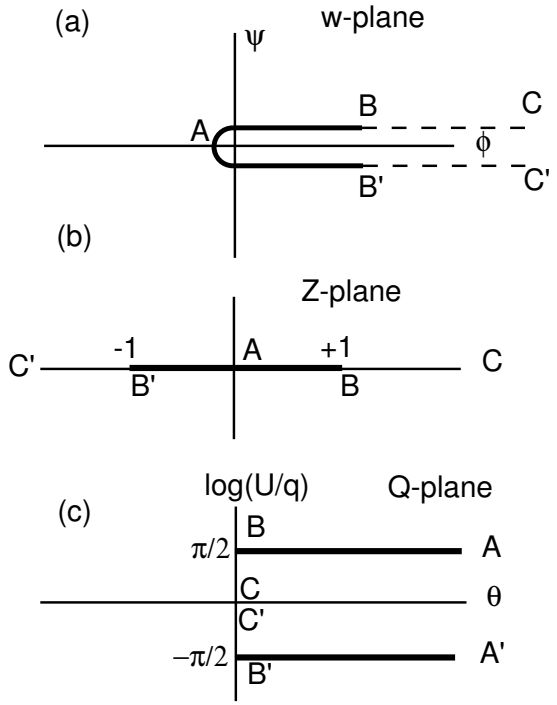

Figure 5.10: The conformal mappings for the Kirchoff solution.

We first note that $w = \phi(x, y) + i\psi(x, y)$, whatever form it may take, maps the z or physical plane shown in figure 5.9 onto the w-plane as shown in figure 5.10(a). The body is here a streamline $\psi = 0$. We next map the w plane onto the Z plane as shown in figure 5.10(b). The map is defined by

$$w = \frac{C}{2} Z^2 \tag{5.23}$$

where the constant C will need to be chosen to make the points B, B' map onto $(1, 0)$ and $(-1, 0)$.

Next, consider the variable

$$Q = \ln \frac{U}{q} + i\theta, \tag{5.24}$$

where $q = \sqrt{u^2 + v^2}, \theta = \tan^{-1} \frac{v}{u}$ with $u - iv = dw/dz$.. The Q plane will be the hodograph plane. The mapping of $Y = 0$ to the hodograph plane is especially simple since either the angle or the speed is constant. Thus we are bound to get a polygon. Since we know how to map a polygon onto the upper half-plane, we can connect Z to Q.

We show the Q plane in figure 5.10(c). The map from z to Q is a Schwarz-Christoffel map, given by

$$\frac{dQ}{dZ} = \frac{1}{Z\sqrt{Z^2 - 1}} \times \text{ constant.} \tag{5.25}$$

The integral may ve calculated using a subatitution $Z = 1/\cosh X$. We obtain

$$Q = C_1 \cosh^{-1} \frac{1}{Z} + C_2 = C_1 \log \Big[\frac{1}{Z} + \sqrt{\frac{1}{Z^2} - 1} \Big] + C_2 = Q(Z), \tag{5.26}$$

where $C_{1,2}$ are constants.

But $Q(e^{i\pi}) = -C_1 i\pi + C_2 = -i\pi/2, Q(1) = C_2 = i\pi/2$, giving

$$Q = \log \Big(\frac{1}{Z} + \sqrt{\frac{1}{Z^2} - 1} \Big) + \frac{i\pi}{2}. \tag{5.27}$$

Since $Q = \log \frac{U}{\frac{dw}{dz}}$ we have using (5.27)

$$U \frac{dz}{dw} = iZ^{-1}[1 + \sqrt{1 - Z^2}]. \tag{5.28}$$

Also $\frac{dw}{dZ} = CZ$, so

$$U \frac{dz}{dZ} = iC(1 + \sqrt{1 - Z^2}). \tag{5.29}$$

If the width of the plate is L, then

$$\int_{-1}^{+1} U \frac{dz}{dZ} dZ = iUL = iC \int_{-1}^{+1} (1 + \sqrt{1 - Z^2} dZ = iC(2 + \pi/2). \tag{5.30}$$

This determines C and gives

$$w = \frac{UL}{4+\pi} Z^2. \tag{5.31}$$

Since we also have

$$U^{-1}\frac{dw}{dz} = \frac{iZ}{1+\sqrt{1-Z^2}}, \tag{5.32}$$

we have defined implicitly $w(z)$.

We will now show that, because of the cavity, the plate experiences a drag. The drag is given by

$$D = \int_{plate} pdy = -i\int pdz = \frac{-i\rho}{2}\int (U^2 - q^2)dz. \tag{5.33}$$

Now on the front face of the plate $q^2 = v^2 = \left(\frac{\partial\phi}{\partial y}\right)^2 = -(dw/dz)^2$, and so , using (5.31) and (5.29) we have

$$D = \frac{\rho U^2 L}{2} - \frac{i\rho}{2}\int_{-1}^{+1} (dw/dZ)^2 (dZ/dz) dZ$$

$$= \frac{\rho U^2 L}{2} - \frac{\rho U L}{4+\pi}\int_{-1}^{+1} (1-\sqrt{1-Z^2})dZ = \frac{\rho U^2 L}{2}\frac{4-\pi}{4+\pi} = \frac{\rho U^2 L \pi}{\pi+4}. \tag{5.34}$$

This drag is close to what is observed when a flat plate is placed in a stream and a wake cavity forms. As we have already noted observed bluff body flows are time dependent and of course the cavity is finite in extent. Nevertheless the Kirchoff solution is a classic example of fluid modeling, exhibiting many features of observed flows and providing a good example of the role of free streamlines in the production of drag.

5.5 The 3D wing: Prandtl's lifting line theory

Airplanes and birds fly in three dimensions. We will now explore how lift and drag arise in the real world. Since D'Alembert's paradox now implies neither lift nor drag is possible in irrotational flow, it is clear that lift and/or drag imply the existence of vorticity in the fluid.

We start by reviewing the vorticity stucture of a 2D Airfoil, in particular a flat plate at angle of attack with the Kutta-Joukowsky condition applied. We know the complex potential in the flat plate problem from section 5.1:

$$w(z) = W(Z(z)), W(Z) = Q[e^{-i\alpha}Z + a^2 e^{i\alpha} Z^{-1}] - \frac{i\Gamma}{2\pi}\ln Z, \tag{5.35}$$

with

$$Z(z) = \frac{1}{2}[z + \sqrt{z^2 - 4a^2}], \Gamma = -4\pi a \sin\alpha. \tag{5.36}$$

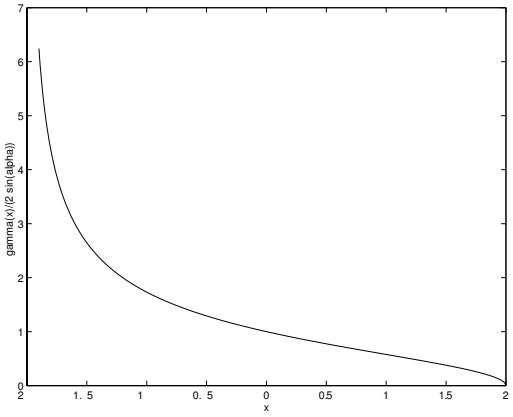

Figure 5.11: The distribution of vorticity on a flat plate, in units of $-2\sin\alpha$.

Since the airfoil has zero thickness, vorticity must be concentrated on the line segment $|x| < 2a, y = 0$. Now $v = 0$ on the segment, so the vorticity $\omega = v_x - u_y$ is given by $-u_y$, and we shall see that u is discontinuous on the segment. Thus the vorticity of the flat plate is proportional to $\delta(y)$, and the total vorticity at a given value of x must be computed as $\gamma(x) = -u(x, 0+) + u(x, 0-)$, with

$$\Gamma = \int_{-2a}^{2a} \gamma(x)dx. \tag{5.37}$$

The plate is therefore said to contain a *vortex sheet of strength* $\gamma(x)$.

Using (5.35) and (5.36), and the fact that $\sqrt{z^2 - 4a^2} = \pm i\sqrt{4a^2 - x^2}$ when $z = (x, 0\pm)$ we obtain (see problem 5.5)

$$u(x, 0\pm) = \pm\sqrt{\frac{2a - x}{2a + x}}\sin\alpha + \cos\alpha, \gamma(x) = -2\sqrt{\frac{2a - x}{2a + x}}\sin\alpha. \tag{5.38}$$

We show $\gamma(x)$ in figure 5.11.

The vorticity of this foil is said to be *bound* to the foil, meaning that it exists "in the plate" and is not present in the fluid. Suppose now that we consider a three-dimensional wing, as shown in figure 5.12. If the wing is sliced by a plane $y =$ constant, we obtain a 2D airfoil section. For example, it might be a Joukowsky section, with its chord c, thickness, camber, and local angle of attack, all functions of y. The direction y is called the *spanwise* direction. The *wingspan* is here $2b$. Since all of the airfoil parameters can vary down the span, we expect the lifting properties of the wing to be a function of y. We also expect that near the center of the wing, the section AB of the figure 5.13(a), the flow should behave as if the section were approximately a two-dimensional airfoil, with vorticity bound to the foil and carrying an associated circulation and lift. However as we move to the tips of tdhe wing, eventually the section lift must go to zero, if for no other reason than that the section chord goes to zero. Since

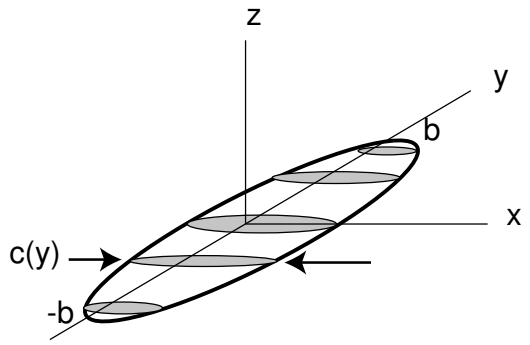

Figure 5.12: The 3D wing.

vorticity is a solenoidal vector, the question has to be, what happens to the vortex lines which were bound to the center section? The answer, suggested in figure 5.13(a), is that the the decrease in the lift distribution as one moves from center to tip, vortex lines turn and are shed into the wake of the wing, thereby reducing the section circulation. Thus there is a sheet of vorticity emerging from the trailing edge of the wing. For many wings the lift decreases to zero rapidly near the tips, so that substantial free vorticity is released near the tips, and this is the source of the "tip vortices" seen in the wake of high-flying jets.

To understand this shedding process, consider figure 5.13(b). We consider a strip of wing sections of width dy. The wing is assumed to be changing so slowly in the spanwise direction that each such strip acts as if it were a 2D airfoil. On this section the lift will then be $l(y)dy$ where $l(y)$ is the 2D lift of the local section. Let the pressure on the upper and lower surfaces be $p_{\pm}(x)$. Then

$$l(y) = -\int_{chord} (p_+(x,y) - p_-(x,y))dx = -\int [p]dy = -\rho U\Gamma(y), \tag{5.39}$$

where $\Gamma(y)$ is the circulation of the local section and the brackets denote the jump from bottom to top surface. Now consider

$$\frac{dl}{dy} = -\int_{chord} \frac{\partial [p]}{\partial y}dx = \int_{chord} \rho \frac{D[v]}{Dt}dx, \tag{5.40}$$

where v is the spanwise velocity component and we are assuming an ideal fluid of constant density. If we assume that the spanwise acceleration is so small that a fluid particles near the wing surface, passing over or under the wing, acquire a spanwise velocity that is small compared to U, then we may substitute $dx = Udt$ and evaluate the last integral as a time integral to obtain

$$\rho U[\Delta v], \tag{5.41}$$

giving the jump in spanwise velocity developed by a fluid particles flowing over the top and bottom surfaces, $\Delta v_{\pm}$ being the spanwise velocities developed at

the trailing edge of the section. Since we expect the lift to decrease as we move toward each tip, the directions of spanwise flow are indicated in figure 5.13(b) for a piece of the left wing looking upstream from the rear of the wing. Since the pressures are *increasing* on the upper surface toward the tip the flow is driven away from the tip. On the bottom surface the spanwise flow is in the opposite direction (the dotted arrow in figure 5.13(b), since on this surface loss of lift is associated with a *decrease* in pressure.

We thus have

$$\frac{dl}{dy} = \rho U \frac{d\Gamma}{dy} = \rho U[\Delta v] \tag{5.42}$$

or

$$\frac{d\Gamma}{dy} = [\Delta v]. \tag{5.43}$$

Here Γ, the circulation on a section, is positive if the spanwise vorticity is in the direction of positive y. Since Γ is the local circulation of a section, (5.43) relates the spanwise change of local lift to the exitence of a discontinuity in spanwise velocity at the strailing edge of the wing.

This discontinuity, $[\Delta v]$, is associated with the production of a vortex sheet at the trailing edge in the x-velocity component $\omega_x = w^y - v_z$. Integrating from $z = 0-$ to $z = 0+$ at the trailing edge, we have $\int \omega_x dz = -[\Delta v]$. This means that $-[\Delta v]dy$ is incremental vorticity shed into the wake at the trailing edge at section y due to the change of l with y. For the left half-wing, as seen from an observer behind the wing looking upstream, $[\Delta v]dy$ is positive if lift increases with y there. Thus $-[\Delta v]dy$ is negative, and so the shed vorticity represents a turning downstream of some of the vortex lines bound to the wing, as shown for $y < 0$ in figure 5.13(a). Similarly, for the right half-wing the decrease of lift with increasing y causes $-[\Delta v]dy$ to be positive.

We now examine the model of the 3D wing created by Prandtl, who sought as a simple means of deducing the lift and drag of a wing, given the section properties of the wing. This model is sometimes called the *lifting line* model. The idea is basically to regard the wing as long and thin. An *aspect ratio* AR can be defined for a wing planform (projection onto the x, y plane) by $AR = \text{wingspan}^2/\text{wingarea} = 4b^2/A$ where b is the half-span. Mathematically, the Prandtl model is an asymptotic approximation to the fluid dynamics of a 3D wing in the limit $AR \to \infty$. The situation is as shown in figure 5.13(c). Because in this limit the chord is small compared to the wingspan, the bound vorticity can be though of as confined to a line, but the circulation about this line becomes a function of y, namely $\Gamma(y)$. If, to fix ideas, ee take each section of the wsing to be a Joukowski foil, then we know from (5.5) that $l(y) = 4\pi\rho c(y)Q^2 \sin(\alpha + \beta)$. We will, along with Prandtl, make the assumption that the angles α, β are small, so that $\sin(\alpha + \beta) \approx \alpha + \beta$ and $Q \approx U$. Then, with the orientation of the coordinate system of 5.13(c) we have, approximately,

$$\Gamma(y) = 4\pi c(y)U(\alpha(y) + \beta(y)). \tag{5.44}$$

We now need to make a crucial reinterpretation of α. Owing to the shed vorticity of the wake, the *effective* angle of attack, that is, the angle made byt the oncom-

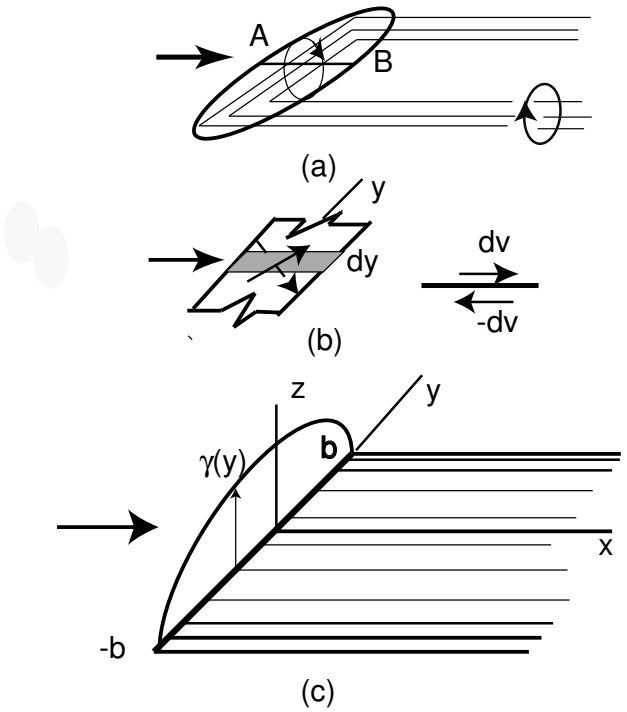

Figure 5.13: (a) The vorticity shed from a 3D lifting wing. (b) The origin of the shed vorticity. (c) Prandtl's lifting line model.

ing stream at the particular section, will be dependent upon the z-component of velocity induced at that section by the shed vorticity. If this veclocity is $w(y)$, then the (small) effective angle of attack is give by

$$\alpha_{eff} = \alpha + \frac{w}{U}, \tag{5.45}$$

where α is the angle made by the section relative to the velocity at true infinity. In other words, the induced w near the wing, the so called *downwash*, changes the apparent "velocity at infinity" from its true value to α_{eff}, and each section will "see" a different approach angle. [2] Now w is an as yet unknown function of y, while β, c are given functions of y determined by the section properties.

With

$$\Gamma(y) = 4\pi c(y)U(\alpha + \frac{w(y)}{U} + \beta(y)) \tag{5.46}$$

we are now in a position to use the Bior-Savart expression for velocity in terms of vorticity, to determine $w(y)$ from $\Gamma(y)$. Recall the the shed x-component of vorticity at each section is $-d\Gamma(y) = \frac{-d\Gamma}{dy}dy$. Now a doubly-infinite vortex induces a velocity given by the 2D point vortex flow. Such a line, carrying unit circulation, parallel to the x-axis at position $y = \eta$ in the $z = 0$ plane, will induce a velocity

$$\frac{1}{2\pi}\frac{1}{y-\eta} \tag{5.47}$$

at any point y on the bound vortex. Since the shed vortex is only semi-infinite, this induced vorticity is reduced by a factor $\frac{1}{2}$. Since the circulation shed at section η is $-\frac{d\Gamma}{dy}dy$ evaluated at $y = \eta$, we have

$$w = -\frac{1}{4\pi}\int_{-b}^{+b} \frac{\frac{d\Gamma}{dy}(\eta)}{y-\eta}d\eta. \tag{5.48}$$

Thus, from (5.46) we obtain

$$\Gamma(y) = 4\pi c(y)U\Big[\alpha + \beta(y) - \frac{1}{4\pi U}\int_{-b}^{+b} \frac{\frac{d\Gamma}{dy}(\eta)}{y-\eta}d\eta, \tag{5.49}$$

which is an integral equation form $\Gamma(y)$.

The beauty of this model is the direct insight it gives into an important fact about three-dimensional aerodydnamics, namely the creation of drag in a perfect fluid model. Observed that whenever the $w(y)$ is negative, which is generally the case for normal wings, the effective angle of attack is less than α. Since our 2D airfoil theory tells us that the local lift is perpendicular to the "flow at infinity", here the apparent or effective flow at infinity, we see that the local lift vector is rotated slightly so as to produce a component in the direction

[2] If $\frac{d\Gamma}{dy} \geq 0$ on the left half-wing and $\frac{d\Gamma}{dy} \leq 0$ on the right half-wing, then, then the shed vorticity is such as to make $w(y) \leq 0$ everywhere at the lifting line, hence the term "downwash".

of positive x. This is a drag component, and the summation over all sections will give rise to the wing drag. This drag, since is is caused by the downwash induced at the wing sectionn by the vortical wake, is called the *induced drag*.

We now indicate how to solve the integral equation (5.49) and calculate the lift and induced drag of our 3D wing. We set $y = -b\cos\theta, 0 \leq \theta \leq \pi$, and suppose that Γ is an even function of y, so it can be is represented by a Fourier series

$$\Gamma = Ub\sum_{n=0}^{\infty} B_{2n+1}\sin(2n+1)\theta. \tag{5.50}$$

Then

$$\frac{d\Gamma}{dy}dy = \frac{d\Gamma}{d\theta}d\theta = Ub\sum_{n=0}^{\infty} B_{2n+1}\cos(2n+1)\theta d\theta. \tag{5.51}$$

Using this in (5.49) we obtain the definite integral

$$\int_0^{\pi} \frac{\cos m\theta'}{\cos\theta - \cos\theta'}d\theta' = -\pi\frac{\sin m\theta}{\sin\theta}, \tag{5.52}$$

The verification of which we leave as problem 5.6. Thus, if $c(y) = C(\theta)$ and $c(y)[\alpha\beta(y)] = D(\theta)$, (5.49) becomes

$$b\sum_{n=0}^{\infty} B_{2n+1}\sin\theta\sin(2n+1)\theta$$

$$-\pi C(\theta)\sum_{n=0}^{\infty}(2n+1)B_{2n+1}\sin(2n+1)\theta = 4\pi D(\theta). \tag{5.53}$$

Given $C(\theta)$ and $D(\theta)$, we are in a position to express all terms as Fourier series in $\sin(2n+1)\theta$ and solve the resulting linear system for the B_{2n+1}.

Given a solution the lift is

$$L = \rho U\int_{-b}^{+b}\Gamma(y)dy = \rho Ub\int_0^{\pi}\Gamma(\theta)\sin\theta d\theta = \frac{\pi}{2}\rho U^2b^2B_0. \tag{5.54}$$

From small w/U, then *induced drag* is given by

$$D_{ind} = -\rho\int_{-b}^{+b} w\Gamma dy = \frac{\pi}{8}\rho U^2b^2\sum_{n=0}^{\infty}(2n+1)B_{2n+1}^2. \tag{5.55}$$

Problem set 5

1. (a) Verify (5.4). (b) Verify that for the Joukowsky family of airfoils the lift is given by (5.5), and that the change comes from the new value of the circulation as determined by the K-J condition.

2. Consider the Joukowski airfoil with $\zeta_0 = bi$ $a > b > 0$. (a) Show that the airfoil is an arc of the circle with center at $(0, -(a^2 - b^2)i/b$ and radius $(a^2 + b^2)/b$. (b) With Kutta condition applied to the trailing edge, at what angle of attack (zas a function of b)is the lift zero?

3. Let the airfoil parameters other than chord (i.e. k, β) be independent of y, the coordinate along the span of the wing. Also, assume the planform is symmetric about the line $x = 0$ in the $x - y$ plane. Using Prandtl's lifting-line theory, show that for a given lift the minimal induced drag occurs for a wing having an elliptical planform. Show in this case that the coefficient of induced drag $C_{D_i} = 2 \times drag/(\rho U^2 S)$ and lift coefficient $C_L = 2 \times lift/(\rho U^2 S)$ are related by

$$C_{D_1} = C_L^2/(\pi AR).$$

Here S is the wing area and AR is the aspect ratio $4b^2/S$. (Some of the WW II fighters, notably the Spitfire, adopted an approximately elliptical wing.)

4. This problem will study flow past a slender axisymmetric body whose surface is given (in cylindrical polar coordinates), by $r = R(z), 0 \leq z \leq L$. Here $R(z)$ is continuous, and positive except at $0, L$ where it vanishes. By "slender" we mean that $\max_{0 \leq x \leq L} R << L$. The body is placed in the uniform flow $(u_z, u_r, u_\theta) = (U, 0, 0)$. We are interested in the steady, axisymmetric potential flow past the body. It can be shown that such a body perturbs the free stream by only a small amount, so that in particular, $u_z \approx U$ everywhere. On the other hand the flow must be tangent at the body, which implies $\phi_r(z, R(z)) \approx UdR/dz, 0 < z < L$.

We look for a representation of ϕ as a distribution of sources with strength $f(z)$. Thus

$$\phi(z, r) = -\frac{1}{4\pi} \int_0^L \frac{f(\zeta)}{\sqrt{(z - \zeta)^2 + r^2}} d\zeta.$$

(a) Compute $\frac{\partial \phi}{\partial r}$, and investigate the resulting integral as $r \to 0, 0 < z < L$. Argue that the dominant contribution comes near $\zeta = z$, and hence show that $\frac{\partial \phi}{\partial r} \approx \frac{1}{4\pi} \frac{f(z)}{r} \int_{-\infty}^{+\infty} (1 + s^2)^{-3/2} ds$ for $r << L$.

(b) From the above tangency condition, deduce that $f(z) \approx dA/dz$ where $A(z) = \pi R^2$ is the cross-sectional area of the body.

(c) By expanding the above expression for ϕ for large z, r, show that in the neighborhood of infinity

$$\phi \approx \frac{1}{4\pi} \frac{z}{(z^2 + r^2)^{3/2}} \int_0^L A(\zeta) d\zeta, z^2 + r^2 \to \infty.$$

5. Verify (5.38).

6. Verify (5.52). (Suggestion: Let $z = e^{i\theta'}, \zeta = e^{i\theta}$, and convert the integral to one on a contour around the unit circle in the z-plane. You will want to indent the contour at poles on the boundary. Evaluate using residue theory.)

7. The em Trefftz plane is a virtual plane orthogonal to the x-axis in figure 5.13 and placed at large x downstream of the wing. The vortical wake in Prandtl's model may be regarded as intersecting the Trefftz plane on the segment $I : |y| \leq b, z = 0$. The induced drag may be calculated in the Trefftz plane as follows. Adobt the energy balance UD_{ind}, the rate of working doen by the induced drag, is equal to UE, the flux of wake energy through the Trefftz plane (TP). Here

$$E = \frac{\rho}{2} \int_{TP} (\nabla \phi)^2 dy dz, \tag{5.56}$$

where $\nabla \phi = (0, v, w) = (0, \phi_y, \phi_z)$. That is, in the Trefftz plane the velocity perturbations of the free stream are dominated by the induced velocities of the, now doubly infinite line vorticies. Use the fact that $\phi_z = w$ is continuous on Y but ϕ is discontinuous there to show that

$$D_{ind} = -\frac{\rho}{2} \int_{-b}^{+b} w_{TP} [\phi]_{TP} dy, \tag{5.57}$$

where w_{TP} is twice the downwash computed at the lifting line in Prandtl's model, and $[\phi]_{TP} = \phi(y.0+) - \phi(y, 0-)$ on I. From this result show that (5.55) follows from the definition of circulation.